Solid Freeform Fabrication 2024: Proceedings of the 35th Annual International Solid Freeform Fabrication Symposium – An Additive Manufacturing Conference
Reviewed Paper

Effect of two different point-based melt scanning strategies on the microstructure of as-built IN718 parts fabricated via EB-PBF System

S.T Nabil[1,2*], C. Banuelos[1,2], G. Fierro[1,3], M. Madigan[5], S. Tin[5] , E. Arrieta[1,2], L.E Murr[3], R. B Wicker[1,2], F. Medina[1,2]

[1]W.M Keck Center for 3D Innovation, University of Texas at El Paso, El Paso, Texas, 79968

[2]Department of Aerospace and Mechanical Engineering, University of Texas at El Paso, Texas, 79968

[3]Department of Computer Science and Engineering, University of Texas at El Paso, Texas, 79968

[4]Department of Metallurgical, Materials and Biomedical Engineering, University of Texas at El Paso, Texas, 79968

[5]Department of Materials Science and Engineering, University of Arizona, Tucson, Arizona, 85719

Keywords: Microstructure Control, Electron Beam Melting, Scanning Strategy, Inconel 718, Spot Melting

Abstract

Metal additive manufacturing has become integral to the modern aerospace and defense industry. Technologies such as powder bed fusion and direct energy deposition have reshaped these sectors. However, challenges like anisotropy and process-related defects still prevent the direct use of printed parts without post-processing. Electron beam powder bed fusion (EB-PBF) is well known for allowing builds at elevated temperatures and eliminating the need for stress relief. However, EB-PBF parts also experience epitaxial growth in the build direction, which causes anisotropy. This research explores two scanning strategies with spot melting techniques—stochastic and single directional—to fabricate IN718 parts using EB-PBF. After fabrication, the samples were analyzed using EBSD to evaluate grain formation in all directions. The findings suggest that point-based melting, guided by these strategies, can affect the microstructure in the build direction. This advancement offers the potential for tailoring controlled parts in future applications.

1 Introduction

Additive manufacturing in metals has shown the potential to transform the aerospace and defense industry with lightweight and complex structures that were previously difficult to manufacture using traditional methods[1–3]. Materials such as Ti-6Al-4V, AlSi10mg, and nickel-based superalloys like Inconel 718 (IN718) are commonly used in these applications due to their high strength-to-weight ratio and corrosion resistance[4–6].

Despite all the positive sides, AM parts have been shown to exhibit anisotropic mechanical properties due to the layer-by-layer fabrication process and the resulting microstructural

features.[7,8]. This restricts AM parts from being used directly after fabrication and requires post-processing steps such as Hot Isostatic Pressing (HIP) or solution and aging heat treatments to improve the mechanical performance.[9,10].

Inconel 718 is a nickel-chromium-based superalloy used in applications like turbine blades, rocket engines, and spacecraft components. This superalloy is precipitation-hardened and can hold its strength up to 650°C without deformation[11–13]. This alloy also poses directional solidification and susceptibility to cracking during fusion-based AM processes[14,15]. Electron beam powder bed fusion, along with scanning strategies, can allow a cure for this problem[16].

Electron Beam Powder Bed Fusion (EB-PBF) is a powder bed fusion additive manufacturing technique that utilizes a high-energy electron beam to selectively melt metal powder layer by layer. The machines work at elevated temperatures that can significantly reduce thermal stress during fabrication[17,18].

Previous studies in EB-PBF have shown the potential to tailor microstructures using scanning strategies. Researchers have reported the effect of different process variables, such as beam current, scan speed, focus offset, and layer thickness on the porosity and surface roughness of EB-PBF parts[19,20].Moreover, the formation of microstructure is greatly dependent on the local solidification rate ® and thermal gradient (G)[21–23]. Some research has also suggested point-based melt strategies to create restrictions in the solidification path to prevent epitaxial grain formation[24–26]. Some research work also stated that inherited porosity can also restrict the path of epitaxial grain formation and allow equiaxed grain formation[27].

This research focuses on two different point-based scanning strategies, Stochastic Spot melt and single directional spot melt, to understand their effect on the microstructure evolution of IN718 parts fabricated via EB-PBF.The parameters chosen were developed at the university premises in another research activity. The objective was to evaluate these point-based melting strategies and gain insights into the microstructural features formed in the as-built parts to evaluate the possibility of tailoring grain morphology.

2 Methodology

2.1 Powder Characteristics

The powder used in this process was AP&C (GE Additive) IN718 plasma atomized spherical powder with a distribution range of 45-106 microns. As specified by the manufacturer, the powder's D10, D50, and D90 values ranged from 52µm to 73 µm and 105µm, respectively. The powder's flowability was 11sec/50g, and it was sieved multiple times during experimentation.

2.2 Implemented Scanning Strategies

Two scanning strategies- stochastic spot melt and single directional point melt were evaluated during the part fabrication process. These scanning strategies were implemented using PixelMelt Software (Freemelt AB, Sweden) to create these patterns. In the stochastic spot melt strategy, the electron beam scans the powder bed in a random pattern during the melt, while in the single directional point melt, the laser scans the powder bed in a unidirectional pattern across the entire layer, as shown in Figure 1.

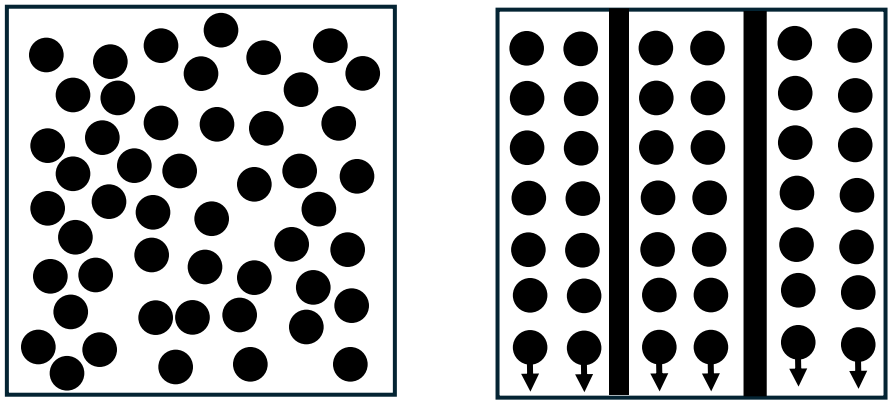

Figure 1: (a) Stochastic Spot Melt; (b) Single Directional Spot Melt

2.3 Fabrication Process and EB-PBF System

FreemeltOne EB-PBF machine (Freemelt AB, Sweden) was used for 15mmx15mmx10mm part fabrication, shown in Figure 1. The machine uses a CO_2 laser to heat up the cathode (LaB6) in a vacuum and uses an electron beam to melt metal powders layer by layer. The machine operates at 60kV in a vacuum with base pressure ranging from 10^{-6} torr to 10^{-7} torr. The maximum beam power for this machine is 6kW. The print process for the FreemeltOne is divided into four stages, namely startheat, preheat, melt and postheat, which are executed sequentially in each cycle during printing.

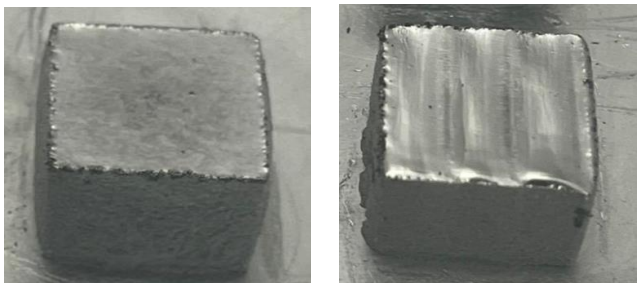

Figure 2: Stochastic Spot Build (Left) ; (b) Single Directional Spot Melt Build (Right)

2.4 Build Parameters

For each of the build the layer height was kept at 75microns – and was chosen based on D50 value from the powder characteristic. The Energy per area spot (Eas) was kept between 9-9.49J/mm^2 for both scan builds. Power was kept at 600W and dwell time was kept between 250-275 microseconds during part fabrication for both scanning strategies. The build plate was heated upto 1050°C measured with thermocouple attached to bottom of the build plate. For stochastic melt the spots were randomized and for single directional spot melt spots moved single directional with a jump length of 5mm.

2.5 Microstructure Analysis

The printed samples were sectioned, mounted, ground, polished, and analyzed using a scanning electron microscope (SEM) for Electron Backscattered Diffraction data(EBSD) to observe the microstructural effects.

3 Results and Discussions

3.1 Microstructural Analysis

The EBSD analysis was done in three directions: XZ, YZ, and XY, where XZ and YZ are parallel to the build direction, and XY is perpendicular to it.

3.1.1 Stochastic Spot Melt Build

Figures 3 and 4 show the EBSD micrographs and pole configurations analyzed for stochastic spot melt builds.

Results perpendicular to the build direction (XY) show a uniform equiaxed microstructure as seen in Figure 3. The pole configuration in Figure 4 displays a random distribution of orientation, with {100} being dominant.

On the other hand, results parallel to the build direction (XZ and YZ) as seen in Figure 3 exhibit a mixture of columnar and equiaxed grains, denoting a columnar to equiaxed transformation (CET). The pole configuration in Figure 4 in both XZ and YZ shows a mixed distribution of {100}, {110}, and {111} orientations, with the XZ direction having a higher density observed in all orientations compared to the YZ direction.

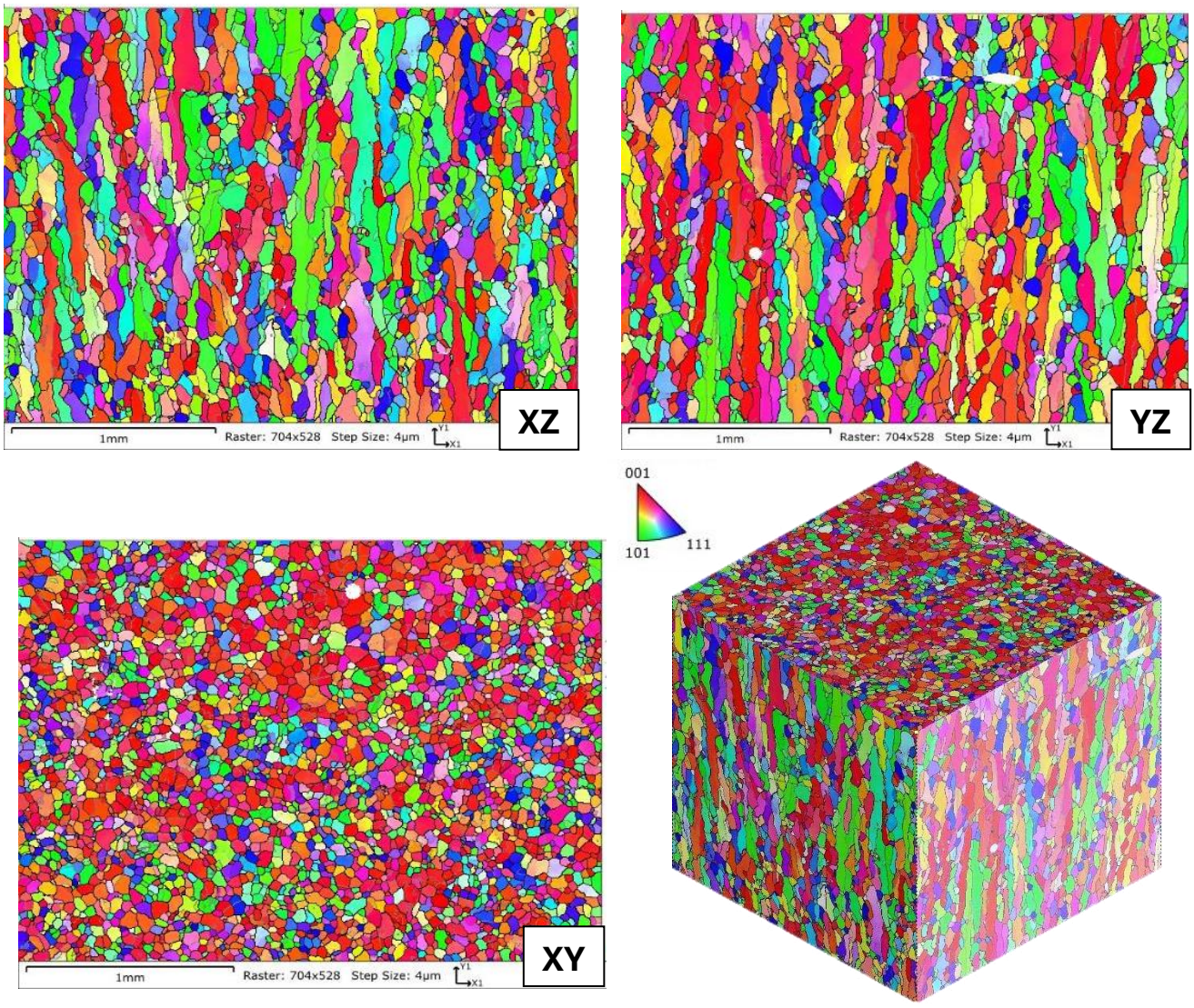

Figure 3 EBSD micrographs analyzed for stochastic spot melt build

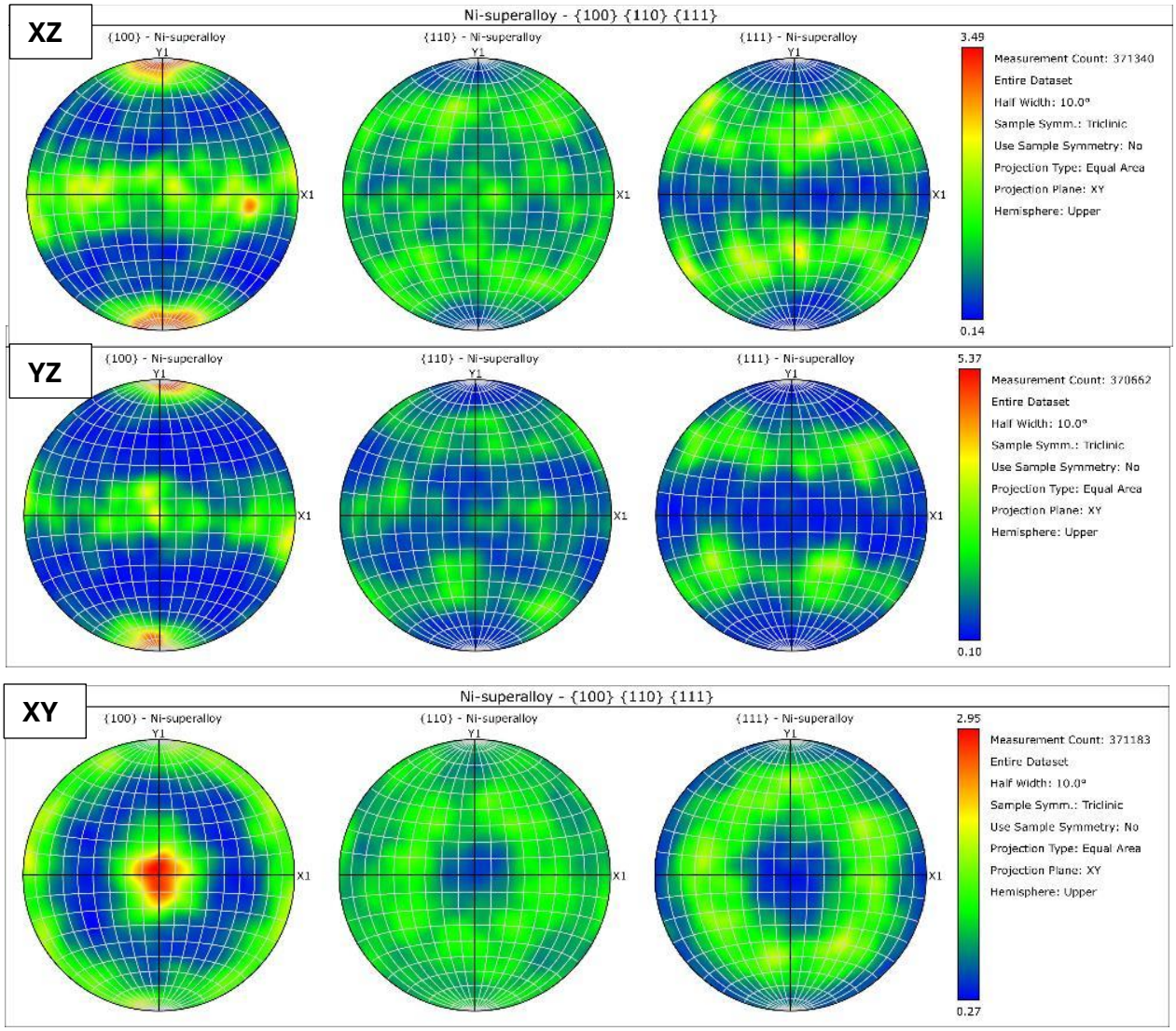

Figure 4 Pole Configuration micrographs analyzed for stochastic spot melt build

3.1.2 Single Directional Point Melt Build

Figure 5 and Figure 6 represents the EBSD micrograph and Pole configuration for the single directional point melt build.

Observing the results perpendicular to the build direction in Figure 5 (XY) shows a mix of larger equiaxed grains and smaller equiaxed grains with a random orientation distribution. The pole configuration for the XY plane in Figure 4 displays a random distribution of orientation, with {100} being dominant.

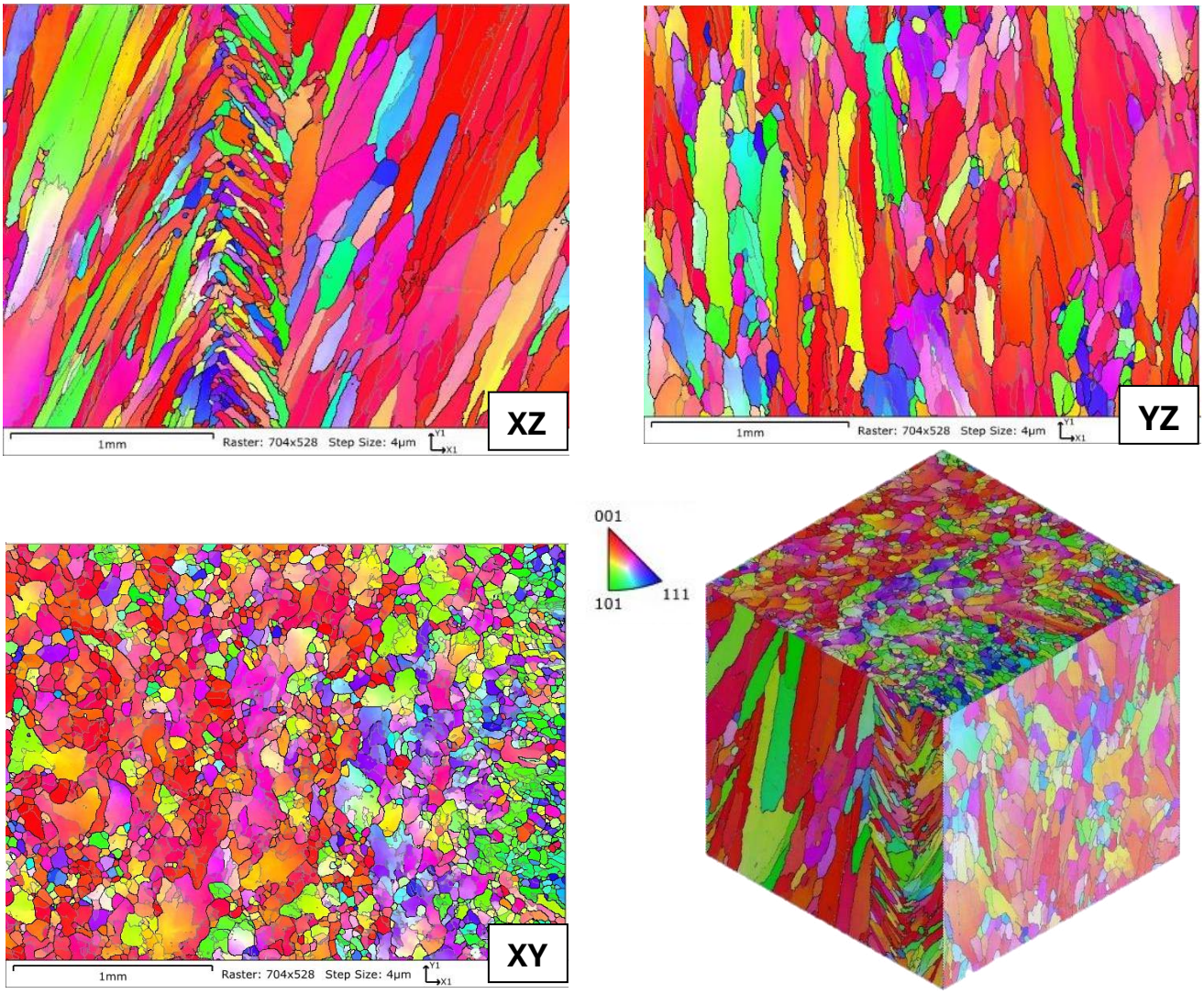

Figure 5 EBSD micrographs analyzed for Single Directional spot melt build

However, directional solidification is prominent in the planes parallel to the build direction (XZ and YZ), as shown in Figure 5. The pole configurations (Figure 6) for these planes show similarity, with a more intense texture observed in the XZ plane compared to the YZ plane. Additionally, in the XZ plane, the intersection points at the 5mm jump length show the formation of equiaxed grains at the intersection region. This is caused by the restriction in the solidification path, promoting the development of more equiaxed grains.

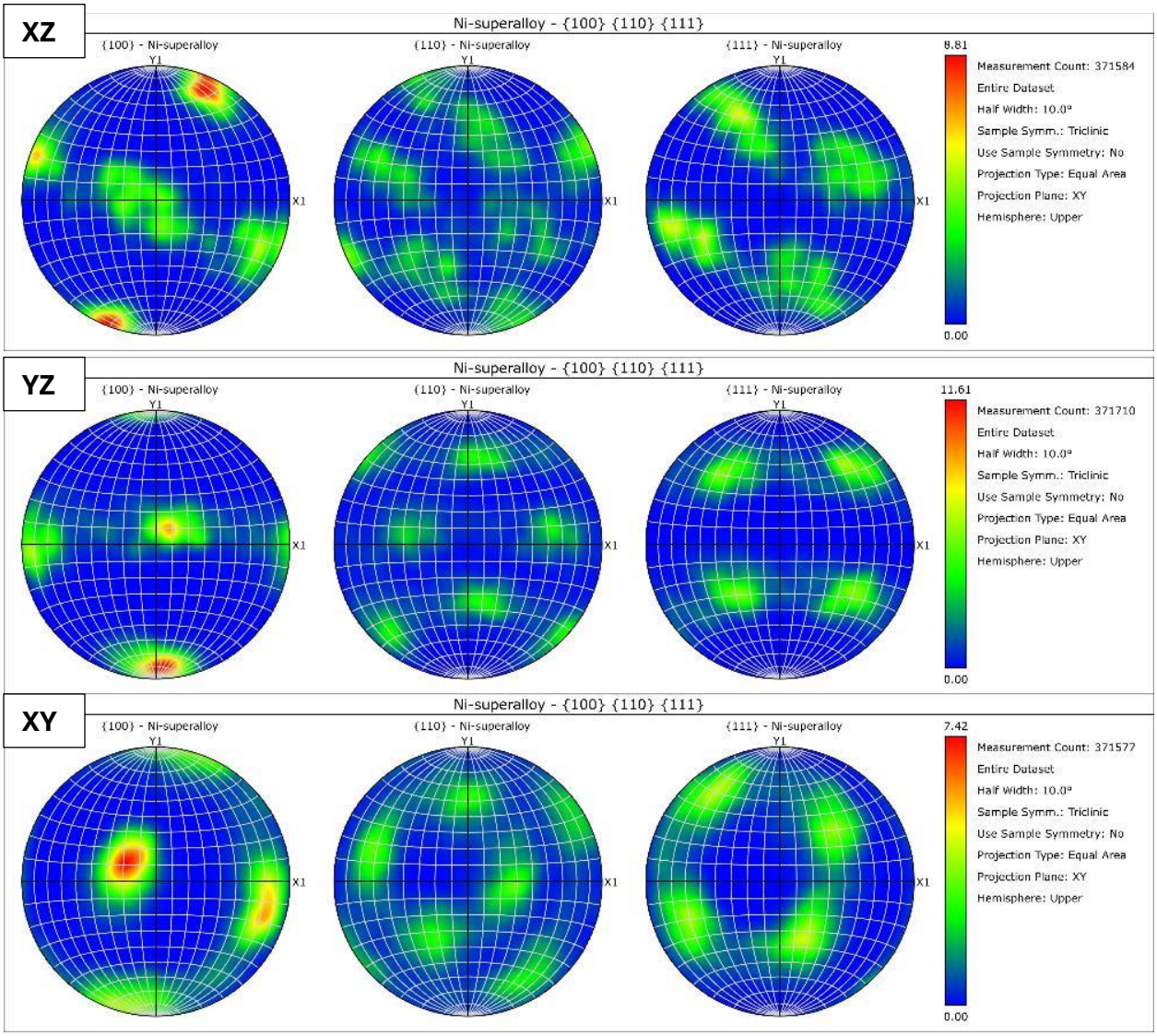

Figure 6 Pole Configuration analyzed for Single Directional spot melt build

3.2 Mean Aspect Ratio and Grain Count

Mean aspect ratio and grain count were obtained from the EBSD result and explain more details in grain morphology as shown in Figure 7(a) and 7(b). Observing the grain count (Figure 7(a)) – stochastic spot melt shows higher grains in all planes: 1590 in XZ, 1332 in YZ and 3515 in XY compared to 567, 521, and 2112 for single directional spot scan. The implementation of stochastic spot scan strategies

Observing mean aspect ratio, stochastic spot scan has lower mean aspect ratio in comparison with single directional spot scan. The single directional spot scan exhibits a higher mean aspect ratio, indicating larger but fewer grains, with values of 3.5 in XZ, 3.6 in YZ, and 1.7 in XY, compared to 2.4, 2.5, and 1.5 for the stochastic spot melt. The higher standard deviation in the single directional spot scan suggests greater grain variability, especially in the XZ and YZ planes, This higher deviation denotes formation of large columnar grains due to the scanning strategy.

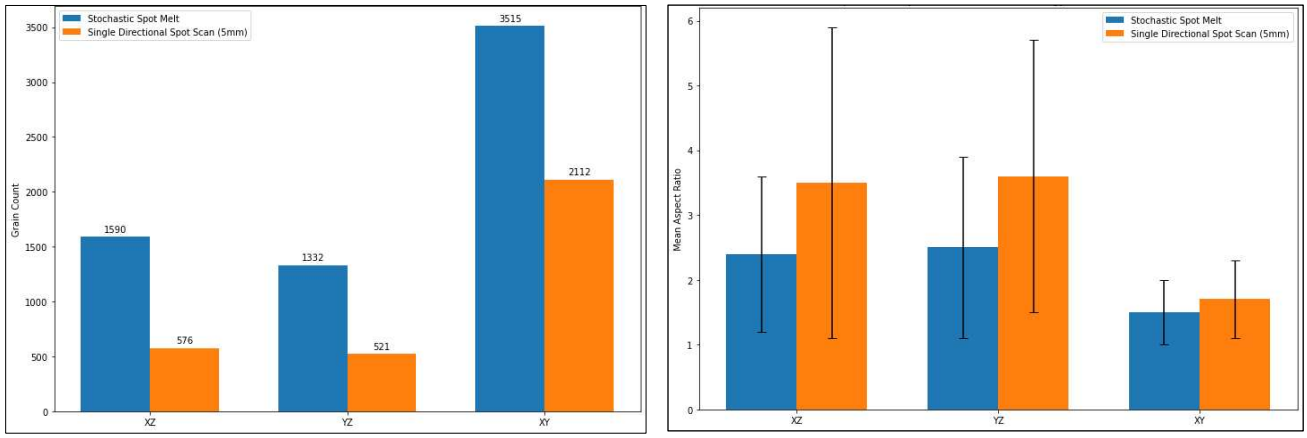

(a) (b)

Figure 7 (a) Grain Count ; (b) Mean aspect ratio for both stochastic and single directional spot

4 Conclusion

This study evaluated analysis of microstructural characteristics and texture evaluation for EB-PBF fabricated IN718 bulk part build with two distinct point-based melting strategy. Overall, the following has been obtained from general observations:

- The stochastic spot melt strategy results in a finer, more uniform grain structure with lower anisotropy.
- The single directional spot scan strategy produces more pronounced anisotropy with larger, columnar grains.
- The stochastic spot melt results higher grain count than single directional spot scan.

These findings underscore the importance of scanning strategies in influencing the microstructure of materials, allowing for the tailoring grain morphology during part fabrication in AM process.

Declaration of competing Interest

The authors declare that they have no known competing financial interests or personal relationships that could have appeared to influence the work reported in this paper.

Acknowledgments

The research presented here was conducted at The University of Texas at El Paso within the W.M. Keck Center for 3D Innovation, a 13,000-sq. ft. State-of-the-art additive manufacturing facility. The fund for this research was provided by the National Science Foundation -Grant Number 2117801. The author appreciates the assistance and opportunities extended by these institutions, which significantly contributed to the completion of this study.

References

[1] B. Blakey-Milner, P. Gradl, G. Snedden, M. Brooks, J. Pitot, E. Lopez, M. Leary, F. Berto, A. du Plessis, Metal additive manufacturing in aerospace: A review, Mater. Des. 209 (2021) 110008. https://doi.org/10.1016/j.matdes.2021.110008.

[2] T. DebRoy, H.L. Wei, J.S. Zuback, T. Mukherjee, J.W. Elmer, J.O. Milewski, A.M. Beese, A. Wilson-Heid, A. De, W. Zhang, Additive manufacturing of metallic components – Process, structure and properties, Prog. Mater. Sci. 92 (2018) 112–224. https://doi.org/10.1016/j.pmatsci.2017.10.001.

[3] J. Boban, A. Puthanveettil Madathil, A. Ahmed, A. Rahman, An overview on post-processing of metal additive manufactured components, in: Mater. Sci. Mater. Eng., [S.I.], 2024. https://doi.org/10.1016/B978-0-323-96020-5.00241-7.

[4] J.C. Diaz, K. Watanabe, A. Rubio, A. De La Cruz, D. Godinez, S.T. Nabil, L.E. Murr, R.B. Wicker, E. Arrieta, F. Medina, Effect of Layer Thickness and Heat Treatment on Microstructure and Mechanical Properties of Alloy 625 Manufactured by Electron Beam Powder Bed Fusion, Materials 15 (2022) 7767. https://doi.org/10.3390/ma15217767.

[5] S.T. Nabil, E. Arrieta, R.B. Wicker, M. Benedict, F. Medina, Effect of Thermal Aging in the Fatigue Life of Hot Isostatic Pressed AlSi10Mg Fabricated by Laser Powder Bed Fusion, in: Proc. 33th Annu. Int. Solid Free. Fabr. Symp. – Addit. Manuf. Conf., 2022. http://dx.doi.org/10.26153/tsw/44562 (accessed March 12, 2024).

[6] C. Banuelos, B. Ramirez, A. De la Cruz, S.T. Nabil, E.G. Arrieta, R.B. Wicker, F. Medina, Fatigue Endurance Investigation of Post-processed Surfaces of LPBF Ti-6Al-4V under Flexural Stress, in: University of Texas at Austin, 2023. https://doi.org/10.26153/tsw/51092 (accessed July 1, 2024).

[7] O. Gokcekaya, T. Ishimoto, S. Hibino, J. Yasutomi, T. Narushima, T. Nakano, Unique crystallographic texture formation in Inconel 718 by laser powder bed fusion and its effect on mechanical anisotropy, Acta Mater. 212 (2021) 116876. https://doi.org/10.1016/j.actamat.2021.116876.

[8] B.E. Carroll, T.A. Palmer, A.M. Beese, Anisotropic tensile behavior of Ti–6Al–4V components fabricated with directed energy deposition additive manufacturing, Acta Mater. 87 (2015) 309–320. https://doi.org/10.1016/j.actamat.2014.12.054.
[9] D.A. Ariza, E. Arrieta, C. Banuelos, B.J. Colón, L.E. Murr, R.B. Wicker, C. Beamer, F. Medina, Comparison of fatigue life behavior between 4-point and uniaxial loading for L-PBF Ti–6Al–4V after HIP treatments, Results Mater. 22 (2024) 100579. https://doi.org/10.1016/j.rinma.2024.100579.
[10] A. Mostafaei, R. Ghiaasiaan, I.-T. Ho, S. Strayer, K.-C. Chang, N. Shamsaei, S. Shao, S. Paul, A.-C. Yeh, S. Tin, A.C. To, Additive manufacturing of nickel-based superalloys: A state-of-the-art review on process-structure-defect-property relationship, Prog. Mater. Sci. 136 (2023) 101108. https://doi.org/10.1016/j.pmatsci.2023.101108.
[11] S.T. Nabil, C. Banuelos, B. Ramirez, A. Cruz, K.I. Watanabe, E. Arrieta, R.B. Wicker, F. Medina, Exploring IN718 alloy production with bi-directional raster and stochastic spot melting techniques using an open-source electron beam melting system, in: Proc. 34th Annu. Int. Solid Free. Fabr. Symp. – Addit. Manuf. Conf., 2023. http://dx.doi.org/10.26153/tsw/44562.
[12] S.S. Babu, N. Raghavan, J. Raplee, S.J. Foster, C. Frederick, M. Haines, R. Dinwiddie, M.K. Kirka, A. Plotkowski, Y. Lee, R.R. Dehoff, Additive Manufacturing of Nickel Superalloys: Opportunities for Innovation and Challenges Related to Qualification, Metall. Mater. Trans. A 49 (2018) 3764–3780. https://doi.org/10.1007/s11661-018-4702-4.
[13] N. Das, Advances in nickel-based cast superalloys, Trans. Indian Inst. Met. 63 (2010) 265–274. https://doi.org/10.1007/s12666-010-0036-7.
[14] S.V. Fortuna, D.A. Gurianov, K.N. Kalashnikov, A.V. Chumaevskii, Yu.P. Mironov, E.A. Kolubaev, Directional Solidification of a Nickel-Based Superalloy Product Structure Fabricated on Stainless Steel Substrate by Electron Beam Additive Manufacturing, Metall. Mater. Trans. A 52 (2021) 857–870. https://doi.org/10.1007/s11661-020-06090-8.
[15] E. Cakmak, M.M. Kirka, T.R. Watkins, R.C. Cooper, K. An, H. Choo, W. Wu, R.R. Dehoff, S.S. Babu, Microstructural and micromechanical characterization of IN718 theta shaped specimens built with electron beam melting, Acta Mater. 108 (2016) 161–175. https://doi.org/10.1016/j.actamat.2016.02.005.
[16] R.R. Dehoff, M.M. Kirka, W.J. Sames, H. Bilheux, A.S. Tremsin, L.E. Lowe, S.S. Babu, Site specific control of crystallographic grain orientation through electron beam additive manufacturing, Mater. Sci. Technol. 31 (2015) 931–938. https://doi.org/10.1179/1743284714Y.0000000734.
[17] Actual state-of-the-art of electron beam powder bed fusion, (n.d.). https://www.tandfonline.com/doi/epdf/10.1080/26889277.2022.2040342?needAccess=true (accessed April 14, 2024).
[18] L.E. Murr, S.M. Gaytan, D.A. Ramirez, E. Martinez, J. Hernandez, K.N. Amato, P.W. Shindo, F.R. Medina, R.B. Wicker, Metal Fabrication by Additive Manufacturing Using Laser and Electron Beam Melting Technologies, J. Mater. Sci. Technol. 28 (2012) 1–14. https://doi.org/10.1016/S1005-0302(12)60016-4.
[19] P. Karimi, E. Sadeghi, J. Ålgårdh, J. Olsson, M.H. Colliander, P. Harlin, E. Toyserkani, J. Andersson, Tailored grain morphology via a unique melting strategy in electron beam-powder bed fusion, Mater. Sci. Eng. A 824 (2021) 141820. https://doi.org/10.1016/j.msea.2021.141820.

[20] X. Ding, Y. Koizumi, D. Wei, A. Chiba, Effect of process parameters on melt pool geometry and microstructure development for electron beam melting of IN718: A systematic single bead analysis study, Addit. Manuf. 26 (2019) 215–226. https://doi.org/10.1016/j.addma.2018.12.018.
[21] W.J. Boettinger, S.R. Coriell, A.L. Greer, A. Karma, W. Kurz, M. Rappaz, R. Trivedi, Solidification microstructures: recent developments, future directions, Acta Mater. 48 (2000) 43–70. https://doi.org/10.1016/S1359-6454(99)00287-6.
[22] Y.S. Lee, M.M. Kirka, R.B. Dinwiddie, N. Raghavan, J. Turner, R.R. Dehoff, S.S. Babu, Role of scan strategies on thermal gradient and solidification rate in electron beam powder bed fusion, Addit. Manuf. 22 (2018) 516–527. https://doi.org/10.1016/j.addma.2018.04.038.
[23] Q. Li, X.-R. Li, B.-X. Dong, X.-L. Zhang, S.-L. Shu, F. Qiu, L.-C. Zhang, Z.-H. Zhang, Metallurgy and Solidification Microstructure Control of Fusion-Based Additive Manufacturing Fabricated Metallic Alloys: A Review, Acta Metall. Sin. Engl. Lett. 37 (2024) 29–53. https://doi.org/10.1007/s40195-023-01656-y.
[24] N. Raghavan, S. Simunovic, R. Dehoff, A. Plotkowski, J. Turner, M. Kirka, S. Babu, Localized melt-scan strategy for site specific control of grain size and primary dendrite arm spacing in electron beam additive manufacturing, Acta Mater. 140 (2017) 375–387. https://doi.org/10.1016/j.actamat.2017.08.038.
[25] A.T. Polonsky, N. Raghavan, M.P. Echlin, M.M. Kirka, R.R. Dehoff, T.M. Pollock, Scan strategies in EBM-printed IN718 and the physics of bulk 3D microstructure development, Mater. Charact. 190 (2022) 112043. https://doi.org/10.1016/j.matchar.2022.112043.
[26] A. Plotkowski, J. Ferguson, B. Stump, W. Halsey, V. Paquit, C. Joslin, S.S. Babu, A. Marquez Rossy, M.M. Kirka, R.R. Dehoff, A stochastic scan strategy for grain structure control in complex geometries using electron beam powder bed fusion, Addit. Manuf. 46 (2021) 102092. https://doi.org/10.1016/j.addma.2021.102092.
[27] X. Ding, Y. Koizumi, K. Aoyagi, T. Kii, N. Sasaki, Y. Hayasaka, K. Yamanaka, A. Chiba, Microstructural control of alloy 718 fabricated by electron beam melting with expanded processing window by adaptive offset method, Mater. Sci. Eng. A 764 (2019) 138058. https://doi.org/10.1016/j.msea.2019.138058.